Extended Abstracts of the 2018 International Conference on Solid State Devices and Materials, Tokyo, 2018, pp501-502

InGaAlAs-InP lateral current injection photonic crystal laser design embedded into the silicon photonics platform

Charles Caër[1], Yannick Baumgartner[1], Marc Seifried[1], Gustavo Villares[1], Herwig Hahn[1], Norbert Meier[1], Daniele Caimi[1], Marilyne Sousa[1], Bert J. Offrein[1], and Lukas Czornomaz[1]

[1] IBM Research – Zurich Research Laboratory
Säumerstrasse 4, Rüschlikon 8803, Switzerland
Phone: +41-44-724-87-80 E-mail: cae@zurich.ibm.com

Abstract

We present a novel design of a CMOS-compatible InGaAlAs-InP photonic crystal laser with lateral current injection embedded in the silicon photonics platform for operation in the O-band. The modelling of the material properties based on our technology and the optical properties of the cavity demonstrates a threshold current of only 70 µA, a maximum output power of 140 µW and a 3 dB frequency response of 27 GHz.

1. Introduction

The integration of light sources on CMOS chips is still a bottleneck of optical interconnects, making the complete integration of III-V lasers on silicon still perceived as a major challenge. While several kinds of III-V on silicon lasers have been reported over the last decade [1,2], the thick stack (several µm) of the III-V materials hinders the integration of such lasers in the back-end of the line (BEOL) of a CMOS chip. For this reason, Lateral Current Injection (LCI) lasers realized in a thin III-V stack are very promising [3,4].

Photonic crystal cavity (PCC) lasers are good candidates for chip-to-chip interconnects and applications requiring low power consumption such as edge computing, since the strong confinement of light in a volume as small as the cubic wavelength ($V \sim (\lambda/n)^3$) enables ultralow threshold current combined with very low junction capacitance [3], and the demonstration of high quality (Q-)factor PCC using deep UV lithography [5] paves a route for a large-scale integration of these devices. However, this type of laser has provided so far very low output power (<< 100 µW), making them unpractical for optical interconnects. Moreover, no CMOS-compatible LCI laser has been demonstrated yet.

We propose in this paper a PCC-LCI laser design based on an InGaAlAs epitaxial stack, which is a quaternary of choice for light emission in the O-band compared to InGaAsP [6,7], thanks to its higher peak gain and characteristic temperature. The MQW stack is then sandwiched by regrown n- and p-InP areas.

2. Laser concept

CMOS-compatible III-V on Si laser embedded between the front-end-of-line (FEOL) and the back-end-of-line (BEOL)

Our approach for the III-V on silicon laser integration relies on thin III-V stack (~ 300 nm) bonded on a SOI wafer and intercalated between the silicon layer (FEOL) and the metal interconnects (BEOL) as drawn in fig. 1 (a). This approach relies on a process including CMOS-compatible metal contacts [8] developed at IBM Zurich and enabled to achieve lasing [9]. The laser cross-section is drawn in fig. 1 (b). The photonic crystal device is made of n-InP and p-InP, while the active region is made of InGaAlAs. The separation of the n- and p-contacts strongly minimizes the leakage current. The active region consists of 10 compressive-strained quantum wells with tensile-strained barriers sandwiched between buffer layers lattice-matched to InP. This heterojunction gives a peak gain of 4000 cm^{-1} (see Appendix). A thin layer of undoped- (u-)InP is grown as a cap layer preventing oxidation of the active region. The n (Sn-doped) and p (Zn-doped) contacts are regrown around the active region. This allows increasing the doping levels to reduce the series resistance (4 times smaller than when using Zn diffusion for a similar resistor length). A thin layer of Al_2O_3 enabling large-scale bonding [10] is located below the seed layer, and the device is fully encapsulated in silicon dioxide (buried oxide and cladding), including the silicon waveguides as well. A heavily doped p+-InGaAs layer is used to provide ohmic contact and is located approximately 2 µm away from the active region as a compromise between the undesired free carrier absorption and the series resistance.

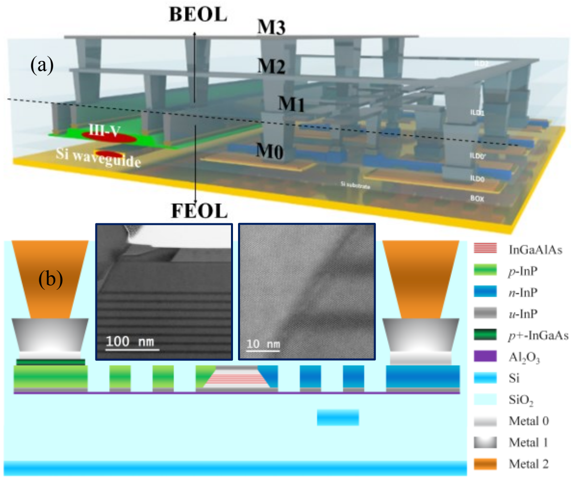

Fig. 1 (a) Schematic showing the concept of the thin III-V active layer fully embedded between the FEOL and the BEOL of an SOI chip. (b) Cross-section of the embedded PCC-LCI with the underlying SOI layer. Insets: STEM pictures of a processed MQW InGaAlAs stack (left) and zoom in on its interface with the regrown InP region (right).

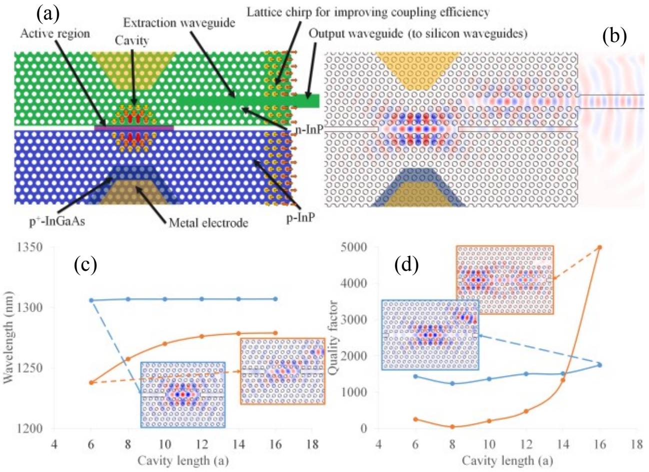

Fig. 2 (a) Drawing showing a top view of the PCC-LCI laser. The white area is filled with silica. (b) Computed fundamental mode of the cavity and its coupling to the output waveguide. (c) Wavelength of the first two modes as a function of the cavity length. (d) Quality factor of the first two modes as a function of the cavity length. Insets show the two modes at different cavity lengths.

Optical Properties of the PCC

The PCC depicted in fig.2 (a,b) consists of a width modulated cavity. The light is extracted by an output waveguide in the n-InP region in order to minimize absorption loss. The first mode of the cavity has a Q-factor of 1450 at λ=1310 nm (fig. 2 (c,d)), which is a good compromise between a short photon lifetime necessary for high-speed modulation and low mirror loss required for the threshold modal gain. Trenches are patterned in order to force carrier to flow into the active region (fig. 2 (a)). These trenches add a "Fabry-Perot-like" resonant mode in the O-band (fig. 2 (c)) but its quality (Q-) factor is too low for short cavities to achieve lasing (fig. 2 (d)), which ensures a single-mode operation.

Plugging the optical properties of the PCC into the rate equations gives a maximum output power of 140 µW at a bias current of 6 mA (fig. 3 (a)), while a threshold current as low as 70 µA (threshold current density of 10.145 kA/cm^2) is obtained. The small-signal response of the laser, including the RC time delay coming from the series and differential resistances and the capacitance, shows a 3-dB frequency response of 27 GHz at the bias current giving the largest wall-plug efficiency (~15 %). The high doping levels enabled by the n- and p-InP regrowth reduces the self-heating and the leakage currents [11]. The developed model used for calculating the laser performances showed its robustness by matching the experimental results of our recent work [9].

3. Conclusions

We have reported a PPCC-LCI laser design demonstrating a sub-100 µA threshold current with an output power exceeding 100 µW. Direct modulation of the laser shows a 3-dB frequency response exceeding 25 GHz. This study demonstrates the potential of high-speed PCC-LCI lasers embedded between the FEOL and the BEOL based on our technology for low-power and low footprint applications.

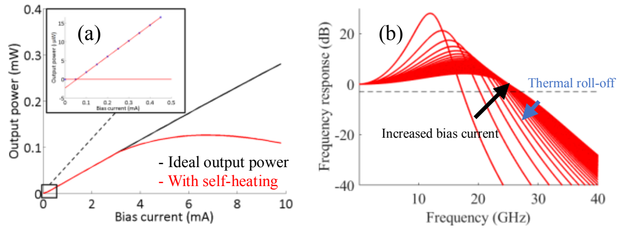

Fig. 3 (a) L-I curve of the PCC-LCI laser, showing a maximum output power exceeding 100 µW. Inset: L-I curve close to the threshold, with linear fits for extracting the threshold current. (b) Small-signal response of the laser with self-heating and a bias current increase.

Acknowledgements

Support from the BRNC OpTeam, the Neuromorphic Devices & Systems and MIND groups at IBM ZRL, and funding from the EU H2020 research and innovation program under grants no. 688003 (DIMENSION), 688172 (ICT-STREAM) and 688544 (L3MATRIX) is acknowledged.

References

[1] G-H. Duan *et al.*, IEEE J. Sel. Top. Quant. Elec. **20** (2014) 6100213.
[2] M. J. R. Heck *et al.,* IEEE J. Sel. Top. Quant. Elec. **19** (2013) 6100117.
[3] S. Matsuo *et al.*, J. Phys. D : Appl. Phys. **47** (2014) 023001.
[4] D. Inoue *et al.*, Opt. Express **23** (2015) 29024.
[5] Y. Ooka *et al.*, Sci. Rep. **5** (2015) 11312.
[6] J. C. L. Yong *et al.*, IEEE J. Quant. Elec. **38** (2002), 1553.
[7] J. Minch *et al.*, IEEE J. Quant. Elec. **35** (1999) 771.
[8] H. Hahn *et al.*, J. Phys. D: App. Phys. **35** (2017) 235102.
[9] M. Seifried *et al.*, *to be published in* IEEE J. Sel. Top. Quant. Elec.
[10] N. Daix *et al.*, APL Materials **2** (2014) 086104.
[11] E. H. Sargent *et al.*, IEEE J. Lightw. Technol. **16** (1998) 1854.
[12] S.-C. Chang, and S. L. Chuang, IEEE J. Sel. Top. Quant. Elec. **1** (1995) 218.
[13] T. Ishikawa and J. E. Bowers, IEEE J. Quant. Elec. **30** (1994) 562.

Appendix

k.p theory is used to calculate the band structure of the InGaAlAs quantum well/barriers stack by diagonalizing a 6x6 Luttinger-Kohn Hamiltonian including a Bir-Pikus potential [12], giving the valence band structure employed in the optical gain calculation, while the conduction band is obtained using the semi-parabolic equation in the effective mass equation. The quasi-Fermi levels are determined self-consistently from the injected carrier density. The calculated gain (g_0=4000 cm^{-1}) includes many-body effects responsible for the bandgap renormalization and Coulomb enhancement for a given injected carrier density [7]. The band structure, gain and optical properties of the cavity are part of a homemade self-consistent model also including rate equations, self-heating and frequency response of the laser, while the PCC properties are calculated by FDTD and PWE methods. The InGaAlAs MQW stack properties are derived from Harrison's model [7,13].